Solar Heat Gain through a Skylight in a Light Well

J. H. Klems

Building Technologies Department

Lawrence Berkeley National Laboratory

Berkeley, CA 94720

Abstract

Detailed heat flow measurements on a skylight mounted on a light well of significant depth are presented. It is shown that during the day much of the solar energy that strikes the walls of the well does not reach the space below. Instead, this energy is trapped in the stratified air of the light well and eventually either conducted through the walls of the well or back out through the skylight. The standard model for predicting fenestration heat transfer does not agree with the measurements when it is applied to the skylight/well combination as a whole (the usual practice), but does agree reasonably well when it is applied to the skylight alone, using the well air temperature near the skylight. A more detailed model gives good agreement. Design implications and future research directions are discussed.

INTRODUCTION

The heat flow through a fenestration system typically is calculated using an equation that conceptualizes the fenestration as a planar, 2-dimensional section of the building envelope surface:

$$W = A_V\left[SHGC(\theta)E_{DN}\cos\theta + \langle SHGC\rangle_D(E_d + E_r)\right] + A_T U \cdot \Delta T \qquad (1)$$

where the "vision" area A_V and the thermal (or "rough opening") area A_T are projected areas in the plane of the envelope surface. (See Appendix A for other nomenclature.) Use of the projected areas in the equation makes it convenient to calculate energy flows based on architectural drawings. The fact that the fenestration in fact has a thickness is accounted for in deriving the value of U to be used in the equation. For normal vertical fenestrations this chiefly consists in doing a 2D heat transfer calculation for the frame and the edge portion of the glazing system. The effects of the three-dimensional nature of the window on the

radiative and convective interior and exterior surface heat transfer coefficients are assumed to be small, and are neglected.

For projecting products, where the departure from planarity is much more significant, application of equation 1 is more problematic. These product have what amounts to a secondary interior space between the actual glazing elements and the aperture in the envelope defined as the "fenestration" in equation 1. It has been shown (Klems 1998) that for projecting "greenhouse" (or "garden") windows the interior surface heat transfer coefficient is significantly modified by this space. Once this has been accounted for, equation 1 can still be used to calculate nighttime thermal energy flows. For daytime solar heat gain, one would expect that it would be significantly more difficult to calculate the performance in a manner that would allow the use of equation 1; however, empirical studies of this issue have not yet been done.

While a "roof window" type of skylight mounted in a cathedral ceiling can be from an energy point of view very similar to an ordinary fenestration in a tilted surface, in the more common installation the skylight sets at the top of a light well that passes through an attic or plenum space. The "rough opening" of equation 1 then becomes the opening at the bottom of the well, where the former joins the architectural space. This may be considered as a projecting product, where much of the projection is in a different space, rather than out of doors. The skylight may, of course, also project above the roof line, as may part of the well, for example, to allow a tilted skylight to be installed on a flat roof.

Equation 1 is usually assumed to be applicable to such a situation. In the thermal calculation the effect of the well is ignored, and the skylight is treated as though it were installed directly in the ceiling of the space. In the case of solar heat gain, it is assumed that all energy admitted by the skylight itself participates in the energy balance of the space. However, it is well known that daylight is attenuated in passing through a long, narrow space such as a light well. Accordingly, a "well daylight efficiency" is assigned to the skylight to account for attenuation in the well. This constitutes the standard modeling of skylights in the DOE-2 building energy simulation program. (Winkelmann, Birdsall et al. 1993)

This paper presents measurements of the heat flow through a skylight with a light well of dimensions that would be reasonable in a residential or office situation. As will be seen, the thermal energy flows are not well described by the above model.

MEASUREMENT PROCEDURE

An accurate, well-characterized and well-known outdoor test facility (Klems, Selkowitz et al. 1982; Klems 1992) was utilized for the measurements. Although normally used to study vertical fenestrations, this facility was designed with ports in its nearly flat roof for the installation of skylights. A commercial skylight adapter for mounting tilted skylights on a

flat roof was attached to each of these ports, and an insulated light well built on the interior. The resulting configuration is shown in Figure 1 and a detailed cross section of the light well in Figure 2. General features of the conversion have been described previously. (Klems 2000; Klems 2001)

Identical flat skylights, each with clear double glazing mounted in an aluminum-clad wood frame, were mounted on the two test chambers. The skylights were units sold for either residential or commercial applications, donated (along with the adapters) for the tests by a skylight manufacturer. The skylight tilt was nominally 20º; the actual angle of the adapter face was 18º. The skylights faced due south, and the facility was oriented so that the normal window sample walls faced north. This was done so that (except during the early morning and late afternoon) the sun would fall on fully guarded walls. While the normal wall openings for vertical samples were heavily insulated and covered with interior heat flux sensors, we nevertheless wished to keep heat fluxes on that area of the envelope as moderate as possible. The test chambers themselves, denoted A and B, respectively, are distinguished by their location in the facility; in these tests, chamber A was due west of chamber B. The chambers are mirror images of one another rather than identical. A large number of tests on them made over the years have not revealed any significant performance differences in the chamber construction. Construction of the light wells within the adapters and ports was also done in as nearly an identical manner as possible, given that construction was by hand on-site, and that there are normal construction tolerances to be dealt with. Weep holes and vents in the skylight frames were sealed during the tests to prevent air infiltration from confusing the results.

Both light wells were painted with an interior flat white paint. The well in Chamber A was then lined with a highly reflecting aluminized plastic film (98% reflectance). This film was intended to minimized the effect of solar absorption in the walls of the well. Each well was instrumented with radiation shielded air temperature sensors on the well centerline; the locations are shown in Figure 2. The well walls are insulated with approximately 50 mm of polystyrene. Thermally the light well may be divided into the portion that projects above the facility roof, termed the upper well, and the portion below the roof line, termed the lower well. The exterior side of the lower well is exposed only to the guard space, which is kept at approximately the same temperature as the test chamber. The exterior side of the upper well is exposed to exterior ambient conditions, but is shaded from the sun by exterior radiation shields, which are not shown in Figure 2. Surface temperature sensors are built into three of the faces of the upper well, and two faces of the lower well.

The measurements were made at our field test site in Reno, NV over a period of three days in July, 1997.

RESULTS

The measured skylight heat flow is shown for the three days of the tests in Figure 3. The facility records a variety of physical conditions as a function of time, and from these the net energy flowing into the calorimeter can be derived from a dynamic net heat balance each 10 minutes. Figure 3 plots each of these measurements as a point for each of the two chambers (gray diamonds, Chamber A; solid black circles, Chamber B). Each of these series of points then traces the measured heat flow as a function of time. Also plotted (as a continuous curve) is the expected heat flow from Equation 1. Energy flows are defined as positive flowing into the chamber; a negative heat flow represents a heat loss. In this calculation the interior temperature T_I is taken to be the chamber (room) mean air temperature, as would be done in a building energy simulation calculation. Since this calculation neglects the effect of the skylight well, and since the two chambers differ only in the reflectivity and emissivity of the skylight well surfaces, the same curve would be calculated for either chamber.

The fact that the heat flows in the two chambers differ from each other and from the expected curve demonstrates that the actual heat flow experienced by the architectural space depends on the effect of the skylight well. This effect can be substantial; as can be seen the peak heat gain for the white-painted, nonspecular well (Chamber B) is around 25% lower than the expected curve. We note that this is a more architecturally realistic situation than the specular well of Chamber A, which was devised to minimize the well effect for subsequent testing.

Unfortunately, for these tests the instrumentation in Chamber A was not functioning ideally. A temperature controller malfunction caused a small oscillation in the chamber air temperature. This in turn appears as an oscillatory heat flow that is superimposed on the data. Although the temperature excursions are generally less than half a degree Celsius, the resulting oscillatory heat flow error has a peak magnitude of up to 120 W. This is responsible for the apparent large scatter of the points for Chamber A at night. Although less apparent, the malfunction continues during the daytime and is responsible for the apparent asymmetry of the daytime peaks. As a result, the data appears "noisy"; one cannot interpret *short-term* deviations from an expected curve as evidence against the model. Long-term deviations, however, would be significant. (See the discussion of Figure 6(a) below.) This problem did not affect Chamber B; while there are some small transient departures of the average air temperature in Chamber B from the set point (25 ºC) during the day, the resulting heat flow measurement errors are small and are not visible in the graph.

Figure 4 shows the measured air temperature near the top of the light well. This was measured with a radiation-shielded thermistor located on the centerline of the light well 0.25 m below the skylight, the uppermost of the temperature sensors shown in Figure 2. Also shown is the measured outdoor air temperature. During the day the air at the top of the well is substantially hotter than both the outdoor air, and the chamber air temperature. While both wells follow the same general pattern, the temperature in the nonspecular well is

considerably hotter. Both show a distinct dip at solar noon, and are not symmetrical about that point; the afternoon peak in temperature is higher than the morning one.

In Figure 5 we have selected July 14, which is typical and for which we have the best data, and we consider the times, respectively 14:30 and 05:00, at which the temperature at the top of the well is at its highest and lowest values. The latter time is before sunrise. At these times we plot the spatial air temperature profiles in the two wells measured by the temperature sensors shown in Figure 2. It can be seen from this plot that during the daytime peak condition the well air is stably stratified vertically, while at night there is a very small adverse vertical temperature gradient. Other studies of the well temperatures show that the stable vertical stratification appears as soon as the net heat flow through the skylight becomes positive.

ANALYSIS OF RESULTS

Figures 4 and 5 are consistent with the following plausible physical picture of thermal processes in the light well. During the night the inner skylight surface is colder than the well air. This situation is unstable with respect to convection, so convective plumes develop. These cause vertical mixing of the well air, which tends to reduce the vertical temperature gradient. The net result is that the air in the well becomes well-mixed vertically, with only a small adverse temperature gradient, as observed. During the day, by contrast, both solar absorption in the skylight glazing and the higher outdoor air temperature make the skylight surface warmer than the chamber air. This sets up a temperature stratification that is stable with respect to convection. Sunlight absorbed in the walls of the well is in part conducted to the adjacent air, which sets up a convective flow that carries the absorbed heat to the upper part of the well. Air in the upper well can transfer heat to the space below only indirectly, by conduction to a surface that in turn radiates to the space. As a result, heat is trapped in the well air. We note that Figure 4 implies that the temperature-driven energy flow through the skylight should always be outward, except possibly for a brief period near sundown. This is in contrast to the simple (and usual) application of Equation 1, which would have the skylight gaining energy by thermal transfer during midday.

In this picture the skylight well acts as a kind of thermal diode, allowing heat loss at night but opposing heat gain during the day.

This picture explains the general shape of the upper well temperature curves in Figure 4. In the morning the sunlight falls on the west wall of the skylight (as well as the north), heating the well air until the rate of heat loss through the skylight glazing and frame equal the rate at which sunlight is being absorbed. Near solar noon, however, more of the sunlight penetrates to the bottom of the well without striking either the east or west walls, so the temperature falls. After solar noon the well air again heats, but now the outdoor temperature has risen (as can be seen in Figure 4), so the well air must reach a higher temperature in order to transfer the same amount of absorbed solar energy outward. Since the well

reflectance is much higher in the specular well the amount of absorbed solar energy is lower, hence the well air temperature is lower overall.

Well Heat Flow

In order to make this physical picture quantitative, an additional effect must be considered. As indicated in Figure 2, the energy flow measured in this experiment, W_{Meas}, is actually the heat flowing across the thermal aperture of the calorimeter chamber, which is effectively the bottom of the well. This differs from W, the energy flow through the skylight and frame, by the heat flow S, through the walls of the skylight well. W_{Meas} and W include, of course, both heat and solar radiation. Since energy flows are defined as positive flowing into the chamber (or skylight well), the energy flow plotted in Figure 3 for the two chambers is really

$$W_{Meas} = W + S \tag{2}$$

Although the light well was highly insulated during these experiments, S is by no means negligible. As can be seen from Figure 2, the exterior of the upper well is in contact with the exterior air and that of the lower well with the air of the calorimeter guard space. The latter is kept at approximately the same temperature as the calorimeter air. We see from Figure 4 that during the day S should be negative, while at night it should be positive for the upper well and very small for the lower.

The well heat flow was calculated as a weighted sum of the heat flow through the individual surfaces of the upper and lower wells:

$$S = \sum_k q_k \cdot A_W^{(k)} \tag{3}$$

where the index k runs over the eight faces of the skylight well (4 upper well, 4 lower well), q_k and $A_W^{(k)}$ are, respectively, the heat flow through and area of the k$^{\text{th}}$ surface, and of course the total well surface area is $A_W = \sum_k A_W^{(k)}$. The individual surface heat fluxes were calculated from a response factor series, (Mitalas 1968; Kusuda 1969)

$$q_k(t) = \sum_n \left[Y_n^{(k)} \cdot \left(T_I^{(k)}(t - n \cdot \delta) - T_B \right) - Z_n^{(k)} \cdot \left(T_O^{(k)}(t - n \cdot \delta) - T_B \right) \right], \tag{4}$$

where $T_I^{(k)}$ and $T_O^{(k)}$ are the time-dependent interior and exterior surface temperatures, T_B is a constant base temperature (25° C) that cancels out of the calculation, δ is the time step size of the calculation (here, 10 minutes) and the response factors $Y_n^{(k)}$ and $Z_n^{(k)}$ were calculated from the properties of the construction. The program WALFERF (Davis and Bull unpub.), which is based on a published calculation (Myers 1980), was used to calculate the response factors. This program had previously been checked against both DOE2

(Building Energy Simulation Group and Solar Energy Group 1993; Winkelmann, Birdsall et al. 1993) and HEATING7 (Childs 1991).

In a subsequent test (Klems 2001) heat flow sensors were installed in two sections of the skylight well wall and the calculation of Equation 4 compared with the measured heat fluxes. On the basis of those tests, we estimate that the level of error in the calculation of S here is 21 W for Chamber A, and 38 W for Chamber B. Since in all the tests S is small at night, the principle contribution to these errors (which are RMS averages over time) is from daytime heat flows.

A Simple Skylight Model

The simplest method of including the skylight well effect is to use Equation 1 to model the skylight heat flow, W, in Equation 2, but to use the local air temperature for the temperature T_1 in that equation, rather than the space air temperature. For each data point, we extrapolated the measured air temperature from the highest measured location, 0.25 m below the skylight surface to the height of the skylight center, using the highest and next highest temperature sensors to estimate the local vertical temperature gradient. The U-factor used in this calculation was calculated with WINDOW4 (Finlayson, Arasteh et al. 1993; Arasteh, Finlayson et al. 1994) and THERM, (Finlayson, Mitchell et al. 1998) using NFRC standard summer conditions.(NFRC 1991) This U-factor, which was also used in the calculation of curve 1 and in Figure 3, did include some effects of the well in that the THERM calculation took into account the effects of longwave radiant exchange in the well enclosure. (We have termed this a calculation "neglecting the well" because it is the sort of calculation that might be done based on an architectural plan that ignores the well geometry. It uses only temperatures outside the well to define its boundary conditions, and once the well characteristics have been used limitedly in the calculation of the U-factor (in a manner similar to the way 2D frame calculations are included), the skylight is then treated as a purely planar object.) The direct normal solar intensity E_{DN} and the total incident flux on the skylight were measured directly; from these measurements the quantity $(E_d + E_r)$ was calculated. The correct value of the solar incident angle and $SHGC(\theta)$ were calculated at each data point from the time and solar position.

Figure 6 compares this model to the measured data and shows the effect of the correction for well heat flow. Data is shown as an hourly plot for July 14, 1997, which is both typical of the data and is the day for which the data are of the best quality. Results are compared separately for each chamber. Three curves are shown. Curve 1 is a repeat of the original calculation of Equation 1 neglecting the skylight well shown in Figure 3; it represents our starting point. Next, in curve 2, is shown the effect of including Equation 2 in this calculation; this shows the effect of the skylight well heat transfer. Finally, in curve 3 the simple model described above is used to calculate W in Equation 2.

The model matches the data very well for the nonspecular well, as can be seen from Figure 6(b). Those regions of the curve that systematically differ from the data are still within the 38W uncertainty range of the well heat flow calculation. For the specular well (Figure 6(a)) the model is also in agreement with the data, although this is less easy to see in the figure

because of the spurious effects of the air temperature oscillation. In the nonspecular well curve 2 shows that heat flow through the well walls accounts for around one-third of the discrepancy between the data and the original Equation 1 calculation neglecting the well.

Detailed Model

We also constructed a detailed U-factor model intended to match the experimental conditions more closely than does the NFRC calculation. We conceptualized the (temperature-driven) heat flow through the skylight as the area-weighted sum of a one-dimensional glazing heat flux and a one-dimensional frame heat flux. The weighting areas were the vision area and the physical interior surface area of the frame, respectively. Each of these one-dimensional heat fluxes was taken to consist of an exterior heat flux depending on exterior conditions and the exterior surface temperature, a "conductance"' heat flux, depending on the interior and exterior surface temperatures of the glazing or frame, and an interior heat flux depending on interior conditions and the interior surface temperature.

The exterior heat flux was calculated from the measured sky temperature, air temperature and wind speed, in addition to the exterior surface temperature. The WINDOW4 equation for convective coefficient as a function of wind speed for a tilted surface was used. For the frame the "conductance" heat flux was calculated using a frame conductance derived from the WINDOW4/THERM U-factor calculation in the simple model. Effectively this conductance includes the correction for 2D conduction at the edge of the glazing. For the glazing the WINDOW4 equations for convective and radiative heat transfer across an air gap were used; the small temperature drop in the glass layers was neglected. The interior heat flux was modeled as (1) a convective part, using the WINDOW4 convective coefficient relation and the local air temperature (extrapolated to the height of the center of the glazing), and (2) a detailed model of radiation between the glazing or frame and the light well. In this model, the light well was divided into 4 parts vertically, and the north, south, east, and west faces were treated separately, resulting in a total of 16 sections. For each section the view factor to the window or frame was calculated, and the net radiative heat transfer was calculated from the interior glazing or frame surface temperature and the well section surface temperature. A given well section was assumed to have a surface temperature equal to the well air temperature interpolated to the height of the center of the well section. (This assumption should slightly overestimate the radiant heat transfer.) The bottom of the well was modeled as a black surface at the mean chamber temperature. (All of the other well surfaces were assumed to have an emissivity of 0.9 for the non-specular well, an 0.03 for the specular well.)

The assumed interior and exterior surface temperatures were iterated to obtain agreement between the calculated exterior, interior, and "conductance" fluxes. Since there is radiant transfer between the inner surface of the glazing and that of the frame, iteration of the two heat fluxes was coupled. The n^{th} iteration of the frame and glazing heat fluxes used the $(n-1)^{st}$ values of the interior and exterior surface temperatures for the frame and glazing. Five iterations were carried out for each data point, and this sufficed to produce agreement of the interior, exterior and "conductance" heat fluxes to better than $0.01 W/m^2$ (generally much less).

The result of this calculation for the nonspecular well is shown in Figure 7, where it is compared with the simple model and with the data. Since both calculations share the same assumptions about convective coefficients and local air temperatures, the differences between them can only be due to the more detailed treatment of radiation. It turns out that the effect of radiative heat flow is small, as can be seen from the difference between the two curves. During the daytime, both calculations match the data about equally well, given the 38W uncertainty in the calculation of *S*. At night, however, *S* is small (as can be seen from the nighttime coincidence of curves 1 and 2 in Figure 6) and the fact that the detailed calculation matches the data there better than the simplified model is significant. This points up the relative importance of interior radiative exchange for the nighttime U-factor, as was also found in the study of greenhouse windows. (Klems 1998)

IMPLICATIONS

This work has two sets of implications, one for building design and the other for improving energy calculations. We consider the design implications first.

It is clear that skylights have the potential of supplying daylight at considerably lower cost in summertime heat gain than is predicted by standardized calculations. Stratification of the air in the skylight well results in the rejection of much heat that the usual calculation would assume is admitted to the space. Even in some cases where there is no light well, stratification of air in the upper part of the space (for instance, in a residential setting) could result in some heat rejection. (It is unlikely, however, that such a situation could approach the conditions of our measurements without severe effects on thermal comfort due to radiation.)

It is also clear that it is very important to insulate the skylight well. The well in our measurements was insulated with 50 mm of polystyrene, and the well heat transfer was still sizable. The experimental setup was most similar to an installation in a commercial building with a conditioned plenum. In this case it is possible that insulation of the well would appear unnecessary, because it separates two conditioned spaces. The opposite is the case; well heat transfer here results in a direct addition to the cooling load. If the plenum were not conditioned, it would still contain HVAC ducting, so that heat added will have a deleterious impact on the cooling load.

In a residential application the situation is more complex if the space adjacent to the skylight well is an unconditioned attic. In a cold climate insulation of the well is likely to be done to prevent winter heat loss, but in milder climates where the principal concern is cooling loads this may be neglected. This is particularly true when the skylight is a later addition. The effect of the level of skylight insulation in these situations depends on the detailed conditions in both the well and the attic (which could be as hot as, or hotter than, the skylight well).

Consciously utilizing the heat trapping properties of a skylight well could yield systems with still better rejection of solar heat for a given amount of daylight than the skylights in this test. For example, venting the skylight during the daytime in summer could yield better heat rejection than found here. Based on our results it seems likely that systems such as tubular skylights, which have proportionately very long wells, together with special provisions for efficient light transfer down these wells, have the potential for providing daylight with very low solar heat load. The daylight transmission system would need to include provisions for rejecting solar infrared, such as selectively reflective coatings. It is also clear that in such systems special attention must be paid to durability issues raised by the temperatures that the upper parts of the systems will experience.

The implications for improving energy calculations are, first, that little new work is needed at the components level. The present tools are adequate for predicting the behavior of skylights, and only a relatively simple model is necessary, provided that the local air temperature is known. This, however, is a difficulty. Present building energy simulation programs use single air node models and cannot predict temperature stratification. Even modeling the light well as a separate space would not produce a very accurate calculation of the skylight heat transfer, because, as can be seen from Figure 5, the air temperature at the skylight is not close to the average air temperature of the well. Further research should be directed toward finding methods of predicting the air temperature near the skylight, and the interior convection surface heat transfer coefficients. It is likely that properly validated computational fluid dynamics (CFD) calculations will be necessary to form a basis for these predictions, since convection is the principal determinant of the temperature distribution within the well.

ACKNOWLEGMENT

This work was supported by the Assistant Secretary for Energy Efficiency and Renewable Energy, Office of Building Technology, State and Community Programs, Office of Building Research and Standards of the U.S. Department of Energy under Contract No. DE-AC03-76SF00098.

The assistance of Velux-America, which provided the skylights and well adapters used in this project, is gratefully acknowledged, and special thanks are due to Roland Temple for his enthusiastic assistance in planning and preparation.

The author is grateful to the members of the MoWiTT technical staff, Dennis DiBartolomeo, Guy Kelley, Michael Streczyn and Mehrangiz Yazdanian, whose diligence in running and maintaining the MoWiTT were vital to the success of this project.

We are indebted to the Experimental Farm, University of Nevada at Reno, for their hospitality in providing a field site and for their cooperation in our activities.

REFERENCES

Arasteh, D. K., E. U. Finlayson and C. Huizenga (1994). WINDOW 4.1: A PC Program for Analyzing the Thermal Performance of Fenestration Products. Lawrence Berkeley National Laboratory, LBL-35298.

Building Energy Simulation Group, L. B. L. and L. A. N. L. Solar Energy Group (1993). DOE-2 Engineers Manual, Version 2.1A. Lawrence Berkeley Laboratory, LBL-11353.

Childs, K. W. (1991). HEATING 7.1 User's Manual. Oak Ridge, TN, Oak Ridge National Laboratory.

Davis, P. K. and J. C. Bull (unpub.). WALFERF.

Finlayson, E., R. Mitchell, D. Arasteh, C. Huizenga and D. Curcija (1998). THERM 2.0: Program Description: A PC Program for Analyzing the Two-Dimensional Heat Transfer Through Building Products. Lawrence Berkeley National Laboratory, LBL-37371 Rev. 2.

Finlayson, E. U., D. K. Arasteh, C. Huizenga, M. D. Rubin and M. S. Reilly (1993). WINDOW 4.0: Documentation of Calculation Procedures. Lawrence Berkeley Laboratory, Berkeley, CA 94720, Technical Report LBL-33943.

Klems, J. H. (1992). "Method of Measuring Nighttime U-Values Using the Mobile Window Thermal Test (MoWiTT) Facility." ASHRAE Trans. **98**(Pt. II): 619-29.

Klems, J. H. (1998). "Greenhouse Window U-Factors Under Field Conditions." ASHRAE Trans. **104**(Pt. 1): Paper no. SF-98-3-1.

Klems, J. H. (2000). "U-Values of Flat and Domed Skylights." ASHRAE Trans. **106**(2): Symposium MN-00-7-3.

Klems, J. H. (2001). "Net Energy Measurements on Electrochromic Skylights." Energy and Buildings **33**: 93-102.

Klems, J. H., S. Selkowitz and S. Horowitz (1982). A Mobile Facility for Measuring Net Energy Performance of Windows and Skylights. Proceedings of the CIB W67 Third International Symposium on Energy Conservation in the Built Environment. Dublin, Ireland, An Foras Forbartha. **III:** 3.1.

Kusuda, T. (1969). "Thermal Response Factors for Multi-Layer Structures of Various Heat Conduction Systems." ASHRAE Trans. **75**(pt. 1): 246-271.

Mitalas, G. P. (1968). "Calculation of Transient Heat Flow Through Walls and Roofs." ASHRAE Trans. **74**(Pt. 2): 181.

Myers, G. E. (1980). "Long-Time Solutions to Heat-Conduction Transients with Time-Dependent Inputs." J. Heat Trans. **102**: 115-120.

NFRC (1991). NFRC 100-91: Procedure for Determining Fenestration Product Thermal Properties (Currently Limited to U-Value). National Fenestration Rating Council, Silver Sping, MD 20910.

Winkelmann, F. C., B. E. Birdsall, W. F. Buhl, K. L. Ellington, A. E. Erkem, J. J. Hirsch and S. Gates (1993). DOE-2 Supplement, Version 2.1E. Lawrence Berkeley National Laboratory, LBL-34947.

FIGURES

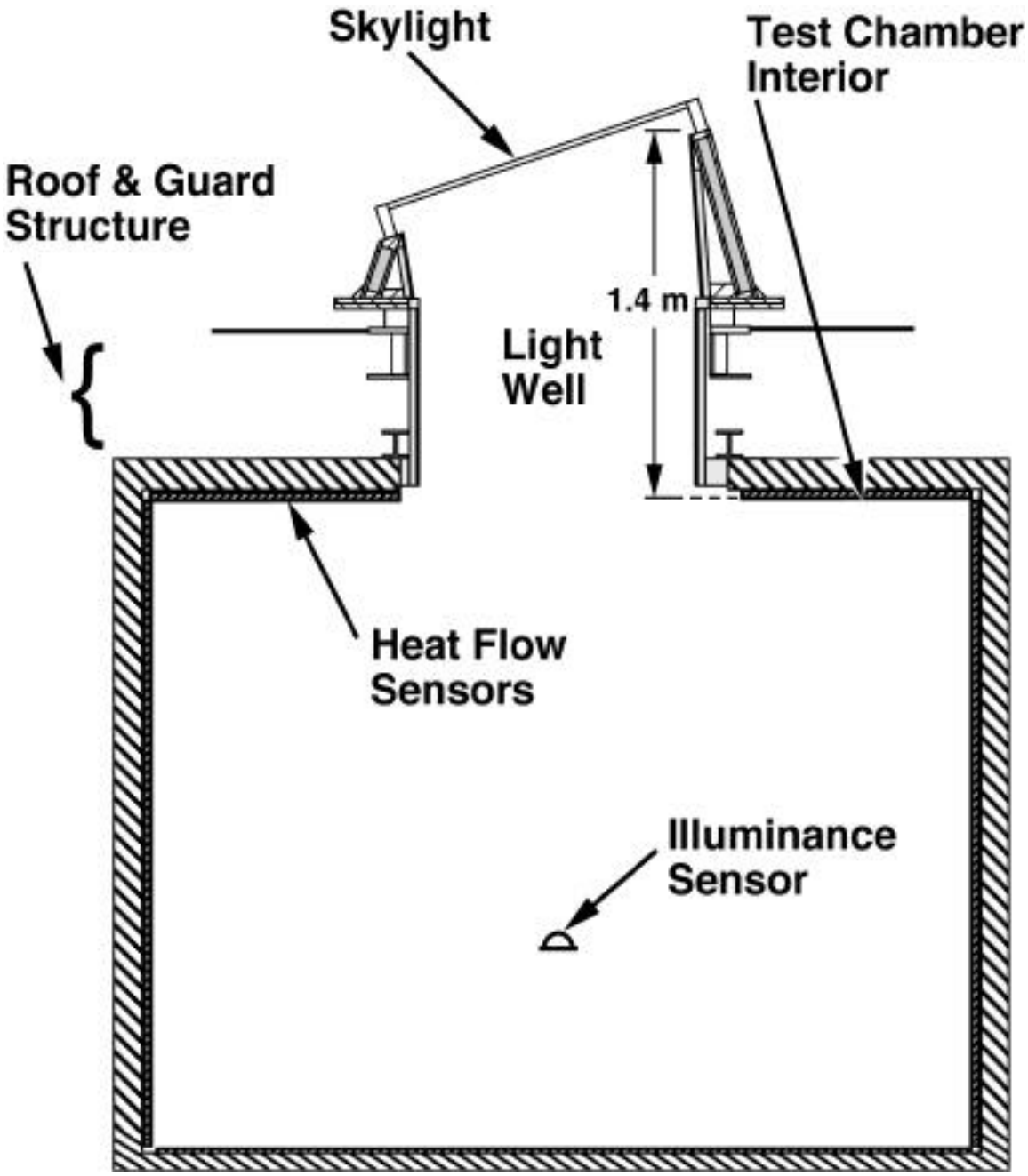

Figure 1. Cross-Section of the Calorimeter Chamber and Light Well. The overall configuration of one of the calorimeter chambers, light well, and skylight mounting is shown in a N-S vertical plane cross-section through the light well center. The interior calorimeter surface formed by the heat flow sensors defines the calorimeter control volume.

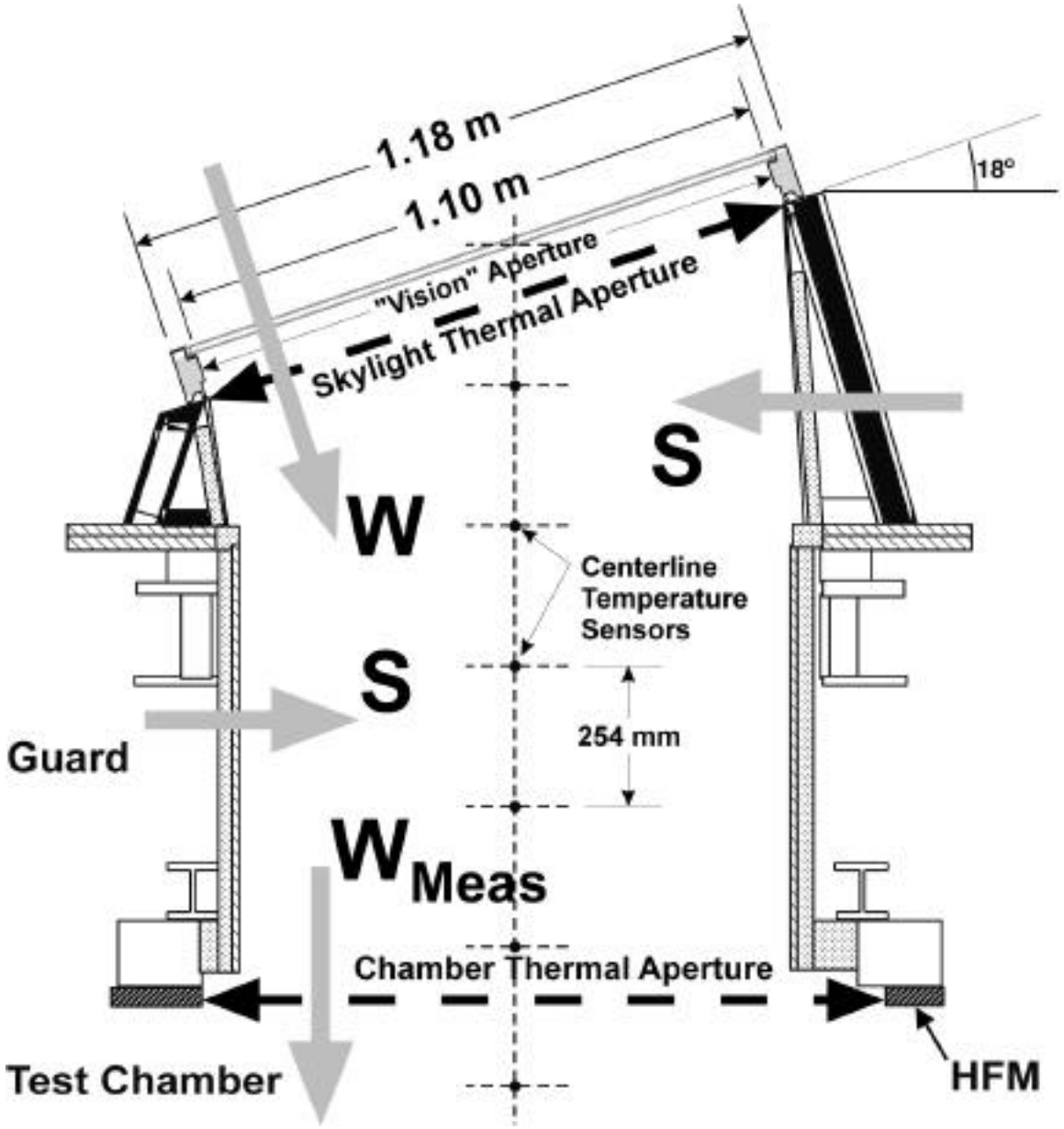

Figure 2. Detail of the Light Well and Skylight. The apertures defining the "vision" area and the skylight thermal area (heavy dashed arrow) are shown, as is the chamber effective thermal aperture (heavy dashed arrow). The heat flow W_{Meas} crossing this aperture and the heat flow, S, through the well sides are illustrated schematically, along with the skylight heat flow, *W*. Also shown are the locations of the well centerline air temperature sensors.

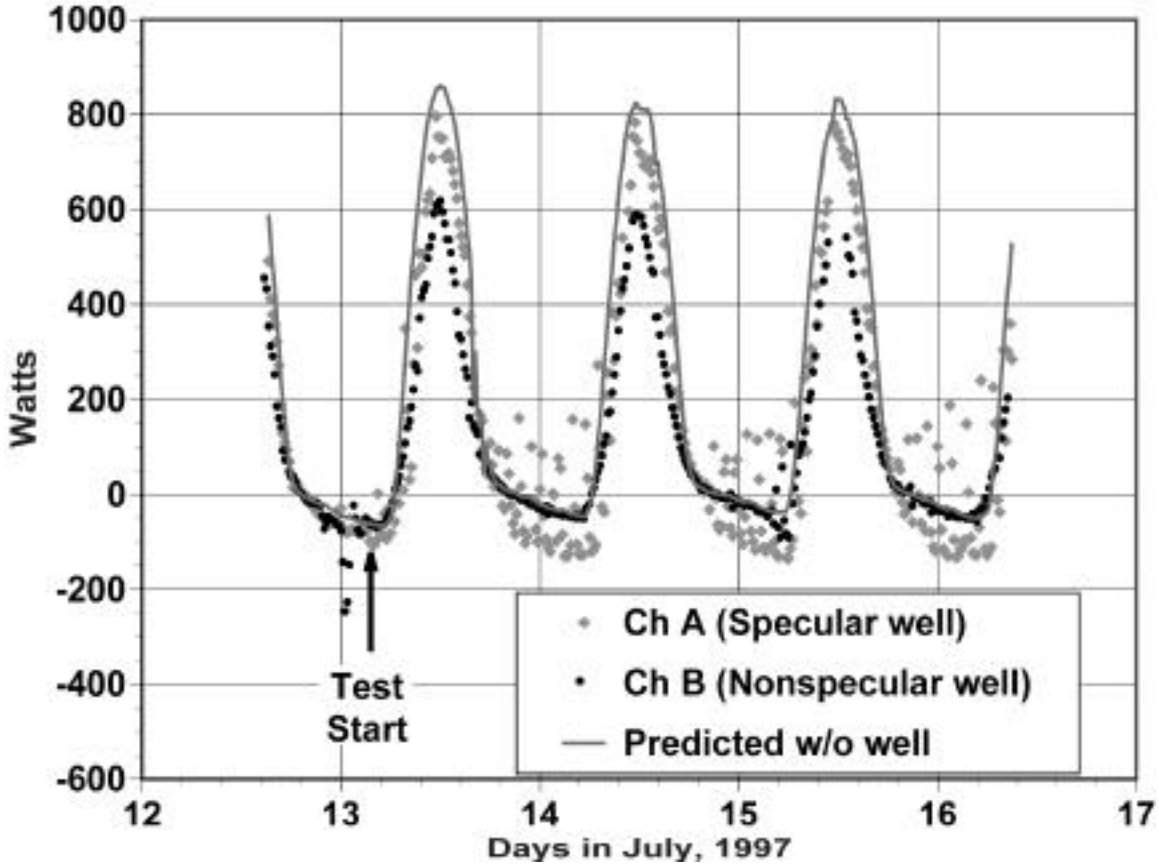

Figure 3. Measured and Expected Heat Flows. The measured heat flows {points: grey diamonds, Chamber A (specular well); black dots, Chamber B (nonspecular well)} in the two chambers are compared with the prediction of Equation 1 (curve), neglecting the effect of the skylight well. The large nighttime scatter apparent in the Chamber A points was due to a malfunctioning temperature controller in that chamber. The sharp excursion in the Chamber B points just prior to the start of the test reflects an entry into the chamber for final preparations. There is a gap in the data around noon on 7/15/97 due to an instrumentation problem.

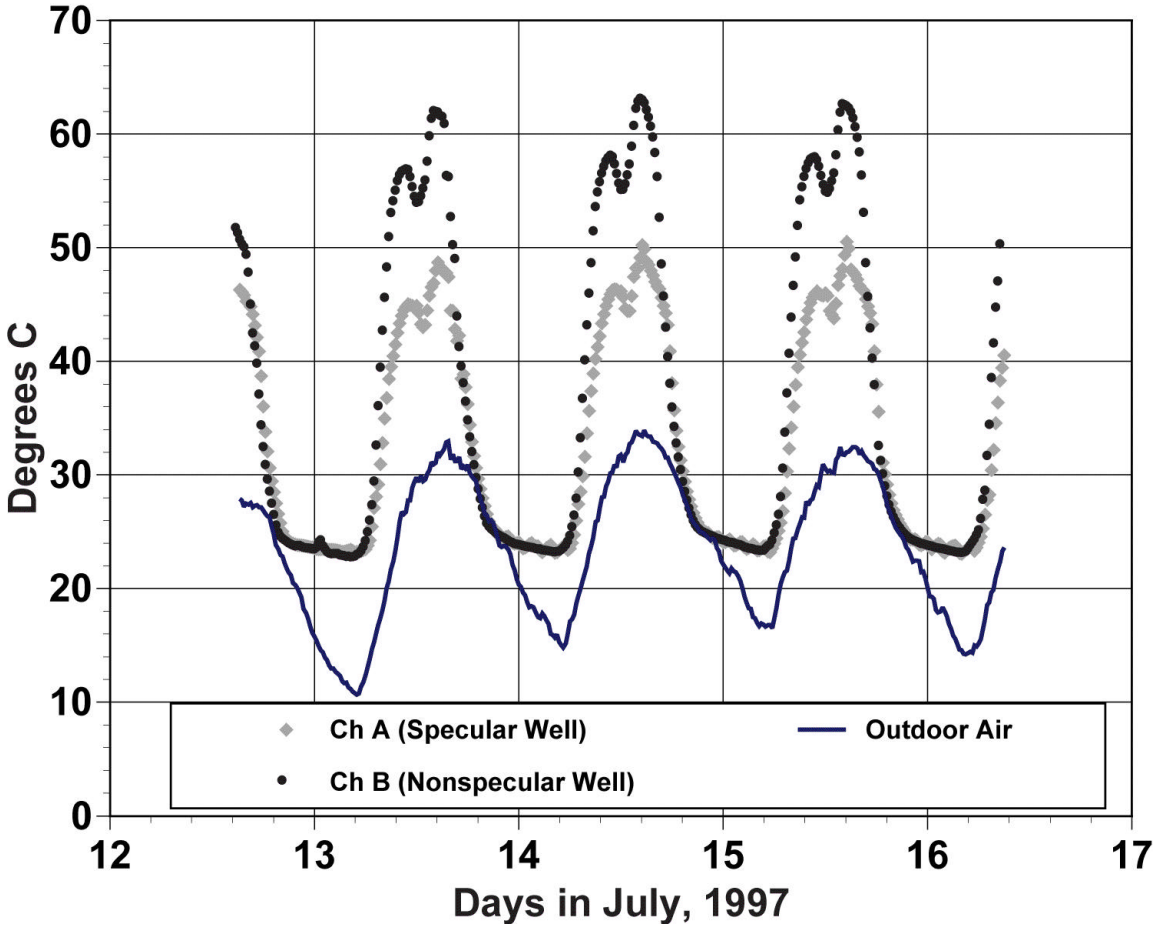

Figure 4. Centerline Air Temperature at the Top of the Light Well. Radiation-shielded temperature sensor is located on the well centerline and 0.25 m below the inner skylight glazing in each chamber. Also shown is the measured outdoor air temperature. The dip in well air temperature at approximately solar noon is associated with the maximum transmission of solar radiation out the bottom of the well without encountering the walls.

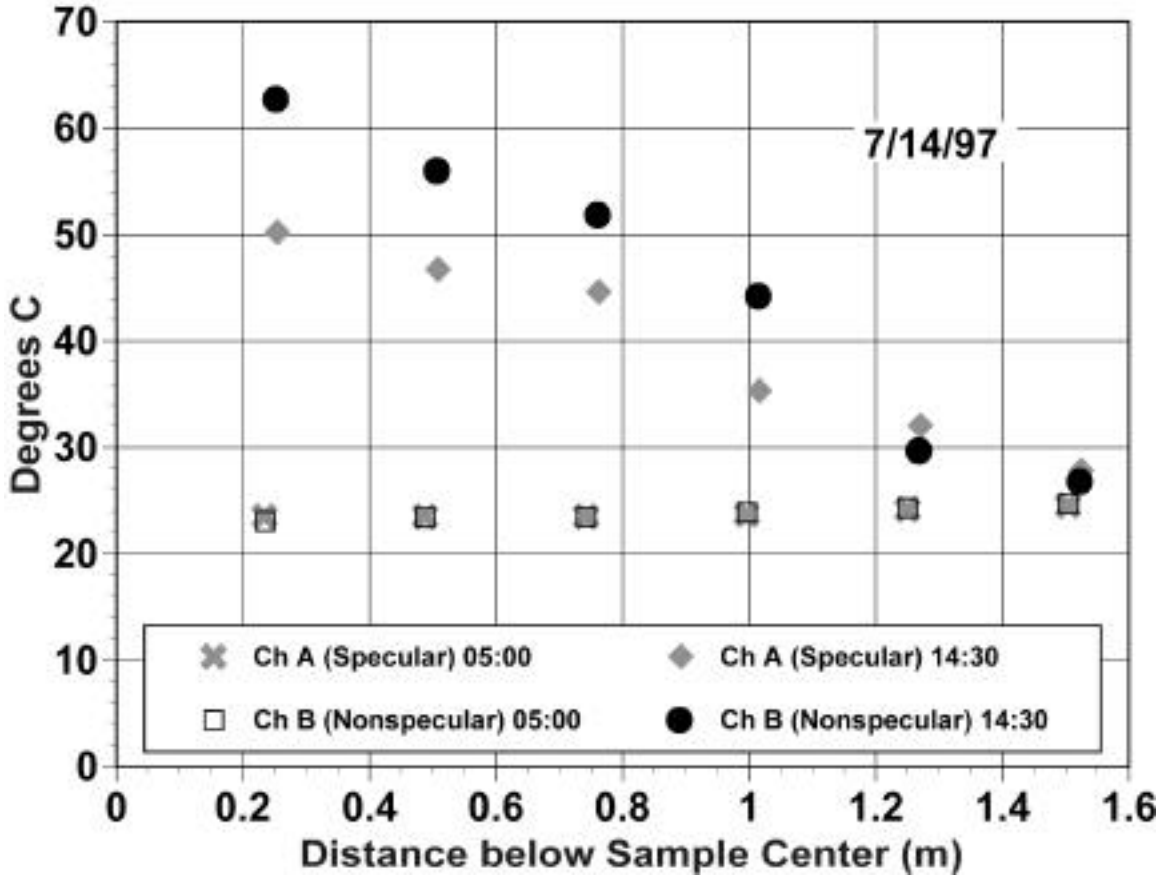

Figure 5. Nighttime and Daytime Well Air Temperature Profiles. Measured air temperatures along the light well centerline at 5 AM and 2:30 PM on July 14, 1997 are shown, relecting nighttime and peak solar gain daytime conditions.

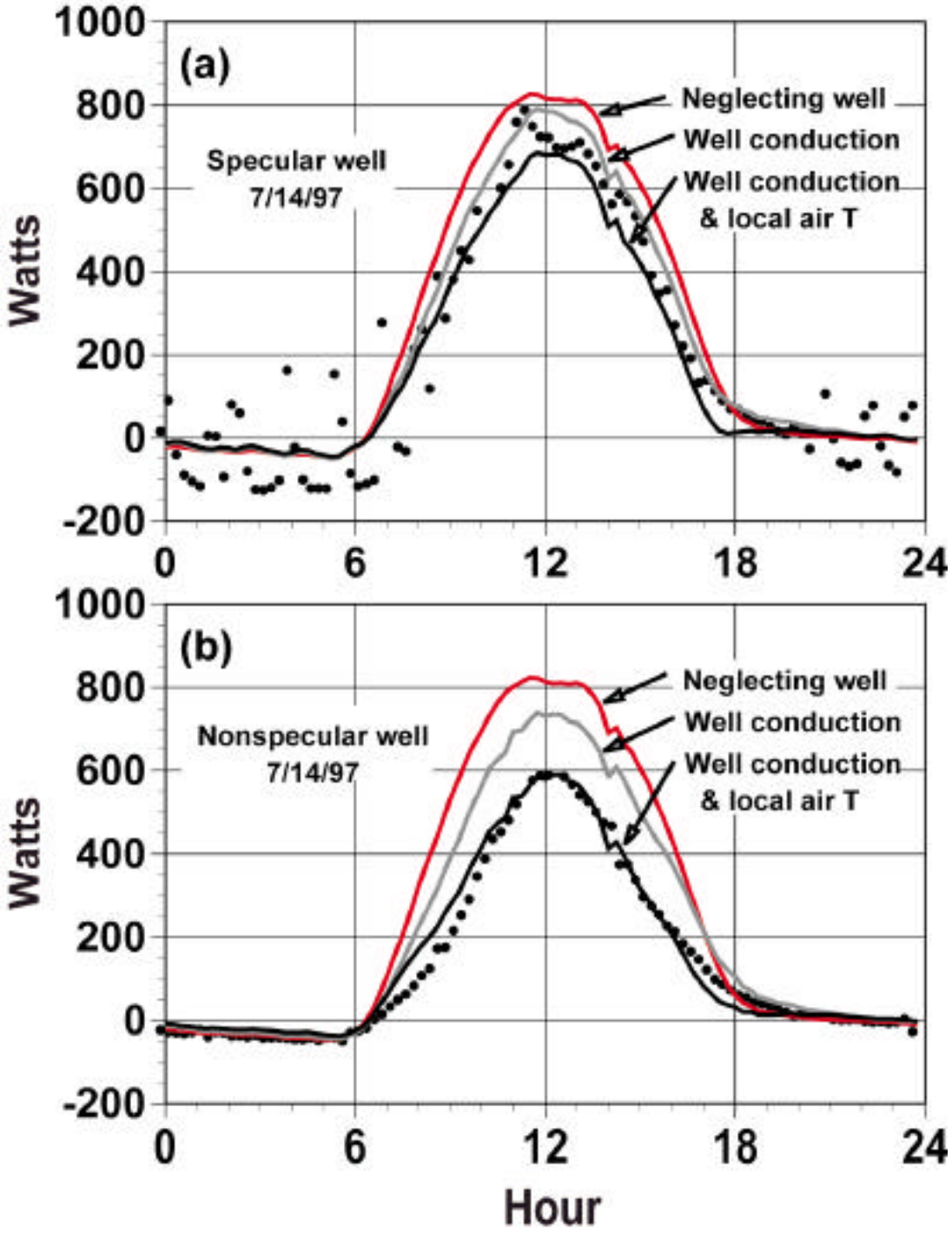

Figure 6. Theoretical Models Compared with Measurements for the Two Light Wells. (a) Specular well (Chamber A), (b) Nonspecular well (Chamber B). The curves plotted are (1)"Neglecting well": Equation 1 calculation using the chamber air temperature and ignoring the effect of the light well; (2) "Well conduction": the same calculation, but adding the heat flow through the well walls by (transient) conduction; (3)"Well conduction & local air T": Equation 1 was applied using the usual U-factor, but the estimated air temperature at the skylight center was used, and the heat flow through the light well walls was added.

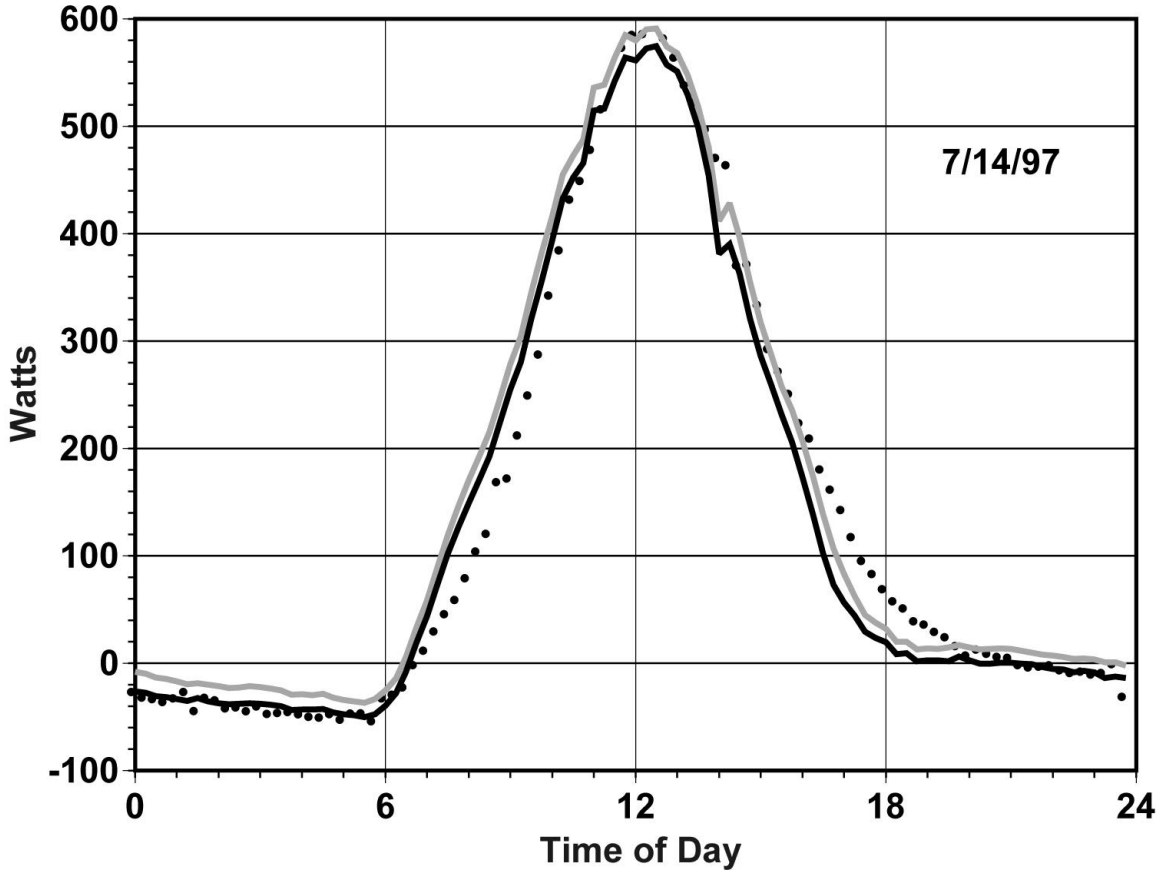

Figure 7. Two Theoretical Models Compared with Measurements, Nonspecular Well. Grey curve: assuming constant (NFRC) U-factor. Black curve: detailed theoretical model of heat flux described in the text. Both curves have the effect of heat conduction through the well walls included.

Appendix A. Nomenclature

Symbols

A_V	Area (projected into the glazing plane) of the transparent ("vision") portion of a fenestration.
A_T	Total ("rough opening") projected area of a fenestration system, including frame.
A_W	Total inside area of the skylight well.
$A_W^{(k)}$	Area of the kth skylight well surface.
E_{DN}	Direct normal solar irradiance.
E_d	Diffuse solar irradiance incident on the fenestration.
E_r	Ground-reflected solar irradiance incident on the fenestration.
θ	Solar incident angle.
q_k	Heat flux through the kth skylight well surface.
$SHGC(\theta)$	Solar Heat Gain Coefficient for incident beam radiation at an incidence angle θ.
$\langle SHGC \rangle_D$	Solar Heat Gain Coefficient for diffuse incident radiation.
T_I	Interior temperature.
T_O	Exterior temperature.
$T_I^{(k)}$	Interior temperature for the kth well surface.
$T_O^{(k)}$	Exterior temperature for the kth well surface.
ΔT	Difference T_O - T_I.
U	Thermal transmittance ("U-factor").
W	Energy flow through the fenestration (here: skylight), defined positive for flow into the space.
$Y_n^{(k)}$	Same-side response factor for the kth well surface.
$Z_n^{(k)}$	Cross-element response factor for the kth well surface.